

# Improved transfer matrix methods for calculating quantum transmission-coefficient

Debabrata Biswas<sup>1</sup> and Vishal Kumar<sup>2</sup>

<sup>1</sup>*Theoretical Physics Division, Bhabha Atomic Research Centre, Mumbai 400085*

<sup>2</sup>*Centre for Excellence in Basic Science, Mumbai University, Kalina, Mumbai 400 098*

(Dated: March 9, 2021)

Methods for calculating the transmission coefficient are proposed, all of which arise from improved non-reflecting WKB boundary conditions at the edge of the computational domain in 1-dimensional geometries. In the first, the Schrödinger equation is solved numerically while the second is a transfer matrix (TM) algorithm where the potential is approximated by steps, but with the first and last matrix modified to reflect the new boundary condition. Both methods give excellent results with first order WKB boundary conditions. The third uses the transfer matrix method with third order WKB boundary conditions. For the the parabolic potential, the average error for the modified third order TM method reduces by factor of 4100 over the unmodified TM method.

## I. INTRODUCTION

The transmission coefficient in quantum mechanics relates the probability flux carried by the transmitted wave relative to the incident wave. It is used in tunneling calculations such as field-emission from metals [1, 2], quantum cascade lasers [3] or more generally when dealing with electron transport at the nanoscale [4–7]. An accurate and computationally effective method to determine this quantity is thus desirable.

In a wide variety of situations where the tunneling region is thin, a 1-dimensional modeling of the tunneling process is adequate. As an example, ultra-thin oxide barriers in metal-oxide-semiconductor (MOS) devices can be modeled using a single degree of freedom. The methods developed in this paper to improve the accuracy of transmission coefficient calculation are of relevance in such quasi 1-dimensional systems.

The WKB formula [8] for transmission coefficient (TC)

$$TC = \frac{e^{-\frac{2}{\hbar} \int_{x_1}^{x_2} \sqrt{2m(E-V(x))} dx}}{\left(1 + \frac{1}{4} e^{-\frac{2}{\hbar} \int_{x_1}^{x_2} \sqrt{2m(E-V(x))} dx}\right)^2} \quad (1)$$

in 1-dimensional systems is the most widely used one in literature. Here  $x_1, x_2$  are the two classical turning points at an energy  $E$  and  $V(x)$  is the potential energy. Eq. (1) is applicable for energies less than the barrier height when tunneling occurs in position space. An analogous WKB formula for above-barrier tunneling can be derived in momentum space at least for simple potentials [8, 9]. While these formulae are easy to use and reasonably accurate at energies for which barriers are broad and high, they are inappropriate for tunneling near the top of the barrier or above-barrier reflection from generic potentials where the momentum space tunneling formula may be hard to implement.

It is thus necessary to rely on numerical methods to determine the transmission coefficient, either by solving the time-independent Schrödinger equation explicitly (referred to hereafter as Differential Equation or DE method) or by approximating the potential by a series

of steps or line-segments and using the transfer matrix (TM) formalism. The step-approximation TM method [10, 11] is one of the most widely used numerical schemes. It is simple to use since the matrix elements are known analytically and it only requires  $N$  matrices to be multiplied where  $N$  is the degree of discretization. Normally, convergence is obtained rapidly with a few thousand matrices.

Both the DE and TM methods mentioned above have an approximation in common [12, 13]. Since numerical methods require a finite domain, they require boundary conditions. This essentially implies that a form for the potential must be assumed beyond the computational domain that is easy to solve so that the wavefunction and its derivative may be matched at the boundary. Normally, it is assumed that the potential is constant beyond the computational domain so that plane wave solutions exist. This allows both the DE and TM methods to be specified fully. For the Schrödinger equation approach (DE), appropriate boundary conditions can be derived while for the transfer matrix method, the boundary matrices can be determined. The results in both cases are generally better than the WKB formula. Our aim here is to go beyond the plane wave assumption mentioned above to provide a non-reflecting truncation scheme for the computational domain and test it by calculating the transmission coefficient.

In Section II, we first review the standard approximation involved in truncating boundaries and then go beyond plane waves by using first order WKB wavefunctions. This is used to derive new boundary conditions for solving the time-independent Schrödinger equation as well as new transfer matrices at the boundary. The first order boundary conditions are implemented numerically in section II C using potentials for which the exact transmission coefficients are known. In Section III, we provide the formalism for third order WKB boundary conditions and implement the same using transfer matrices. Our results are summarized in section IV.

## II. BOUNDARY TRUNCATION USING FIRST ORDER WKB

As mentioned above, a finite computational domain requires boundary conditions that allow flux to be transmitted without causing spurious reflections. In 1-dimensional situations, it is generally accepted that this can be achieved by assuming that the flux beyond is carried away by plane waves. This essentially implies that the potential assumes a constant value on either side of the computational domain. The discontinuity in the first derivative of the potential however requires a reflected wave from the boundary in order that the wavefunctions and their first derivatives match. To see this, let the computational domain be  $L \leq x \leq 0$  with a boundary at  $x = 0$ . For values of  $x$  slightly less than zero, the potential may be approximated by  $V(x) = V(0) - \alpha x$  where  $\alpha = -V'(0)$ . Thus, the Schrödinger equation takes the form

$$-\frac{\hbar^2}{2m} \frac{d^2}{dx^2} \psi(x) - \alpha x \psi(x) = \mathcal{E} \psi(x) \quad (2)$$

where  $\mathcal{E} = E - V(0)$ . For  $\mathcal{E} > 0$ , the solutions are

$$\psi(x) = \begin{cases} \sqrt{z} H_{1/3}^{(1)}(2z^{3/2}/3) \\ \sqrt{z} H_{1/3}^{(2)}(2z^{3/2}/3) \end{cases} \quad (3)$$

where  $z = (\alpha x + \mathcal{E})(2m)^{1/3}(\alpha\hbar)^{-2/3}$  and  $H_{1/3}^{(1,2)}$  are Hankel functions. A general solution in the computational domain near the boundary at  $x = 0$  can thus be expressed as

$$\psi_-(x) = C\sqrt{z}H_{1/3}^{(1)}(2z^{3/2}/3) + D\sqrt{z}H_{1/3}^{(2)}(2z^{3/2}/3) \quad (4)$$

where  $H_{1/3}^{(1)}$  represents a wave moving to the right and  $H_{1/3}^{(2)}$  a reflected wave moving to the left from the computational domain. Matching  $\psi_-(x)$  and its derivative to the plane wave solution for  $x \geq 0$ ,  $\psi_+(x) = F \exp(ikx)$ , leads to a solution where both  $C$  and  $D$  are non-zero. Thus, the plane wave assumption leads to spurious reflection, its magnitude depending on the factors such as the energy  $\mathcal{E} = E - V(0)$ .

There is thus scope to improve upon this truncation scheme. One possibility is to assume that the wavefunction at the end of the computational domain is a first order semiclassical WKB wavefunction

$$\psi_+^{wkb}(x) = \frac{F}{\sqrt{p(x)}} e^{\frac{i}{\hbar} \int^x p(x') dx'} \quad (5)$$

which can be matched at the boundary. The lower limit in the integral in Eq. (5) is an appropriately chosen reference point. We shall build upon this approach first proposed in the context of the self-consistent Schrodinger-Poisson system [14, 15]. Here, as in the plane wave case,

it is assumed that there is no reflection from beyond the computational domain so that a left moving wave is not included in  $\psi_+^{wkb}(x)$ . In addition, it is also assumed that the end of the computational domain is not a classical turning point for the energy considered and that the potential is sufficiently slowly varying over a deBroglie wavelength.

### A. Improved boundary conditions for the Schrodinger Equation (DE method)

For purposes of determining the transmission coefficient, it is easier to write the wavefunction in polar form

$$\psi(\bar{x}) = \left(\frac{JmD}{e\hbar}\right)^{1/2} r(\bar{x})e^{i\theta(\bar{x})} \quad (6)$$

where  $\bar{x} = x/D$ ,  $D$  is the extent of the computational domain and  $r(\bar{x})$  and  $\theta(\bar{x})$  are real valued functions. For convenience in writing the Schrödinger equation in dimensionless form, it is assumed that the tunneling particle is an electron with charge  $-e$  and mass  $m$ . Thus, the tunneling current density is

$$J = \frac{ie\hbar}{2m} \left( \psi^* \frac{d\psi}{dx} - \psi \frac{d\psi^*}{dx} \right). \quad (7)$$

The Schrödinger equation thus reduces to equations for the amplitude and phase:

$$\frac{d^2 r}{d\bar{x}^2} + [(\bar{E} - \bar{V}) - \frac{1}{r^4}]r = 0 \quad (8)$$

$$\frac{d\theta}{d\bar{x}} = \frac{1}{r^2} \quad (9)$$

where  $\bar{V} = V/(eV_s)$ ,  $\bar{E} = E/(eV_s)$  and  $V_s = \hbar^2/(2meD^2)$ . For simplicity, we shall assume the left computational boundary to be at  $x = 0$  and the right boundary at  $x = D$  or  $\bar{x} = 1$ .

Note that once  $r(\bar{x})$  is known,  $\theta(\bar{x})$  can be determined independently with an arbitrary phase ( $\theta(1) = 0$ ) at the right boundary  $\bar{x} = 1$ . The boundary conditions for  $r(\bar{x})$  are easier to implement at  $\bar{x} = 1$ . It is thus simpler to solve Eqn. (8) as an initial value problem starting at  $\bar{x} = 1$ . Our task thus reduces to the determination of  $r(1)$  and  $r'(1)$ .

Using Eqns. (5) and (7), the real coefficient  $F$  can be expressed in terms of the current density  $J$  as  $F = \sqrt{mJ}/e$ . On matching the wavefunctions and their derivatives at  $\bar{x} = 1$ , we have

$$r(1) = \frac{1}{(\bar{E} - \bar{V}(1))^{1/4}} \quad (10)$$

$$r'(1) = -\frac{\bar{V}'(1)}{[4(\bar{E} - \bar{V}(1))^{5/4}]}. \quad (11)$$

In contrast, for a plane outgoing wave,  $r'(1) = 0$ . Eq. (8) can be integrated backward to determine  $r(0)$  and  $r'(0)$ . The transmission coefficient can be obtained by matching  $\psi(\bar{x})$  to the WKB form

$$\psi_-^{wkb}(x) = \frac{A}{\sqrt{p(x)}} e^{\frac{1}{\hbar} \int^x p(x') dx'} + \frac{B}{\sqrt{p(x)}} e^{-\frac{1}{\hbar} \int^x p(x') dx'} \quad (12)$$

at  $x = 0$ . The transmission coefficient can thus be expressed in terms of  $r(0)$ ,  $r'(0)$  and  $\bar{V}'(0)$  as

$$\mathcal{T} = \frac{4}{\left(\frac{r(0)\bar{V}'(0)}{4\bar{\mathcal{E}}^{5/4}} + \frac{r'(0)}{\bar{\mathcal{E}}^{1/4}}\right)^2 + \left(\bar{\mathcal{E}}^{1/4}r(0) + \frac{1}{\bar{\mathcal{E}}^{1/4}r(0)}\right)^2} \quad (13)$$

where  $\bar{\mathcal{E}} = (\bar{E} - \bar{V}(0))$ . An analogous expression for plane outgoing waves can be obtained for comparison.

### B. First Order WKB Transfer Matrices

Solving the Schrödinger equation explicitly using WKB boundary conditions improves computation of the transmission coefficient as we shall see in the next section. Here, we shall investigate whether the popular transfer matrix method can be tweaked to incorporate the WKB truncation technique.

In the transfer matrix method, instead of dealing with a continuous variation of potential and solving the differential equation, the potential is divided into several segments (steps). Each of these segments behaves as an individual potential step and since the segments are small, the potential is considered to be constant for a given segment. The potential tends towards the actual value as the divisions become finer. The open boundary is treated by WKB approximation assuming the potential to be slowly varying outside the computational domain.

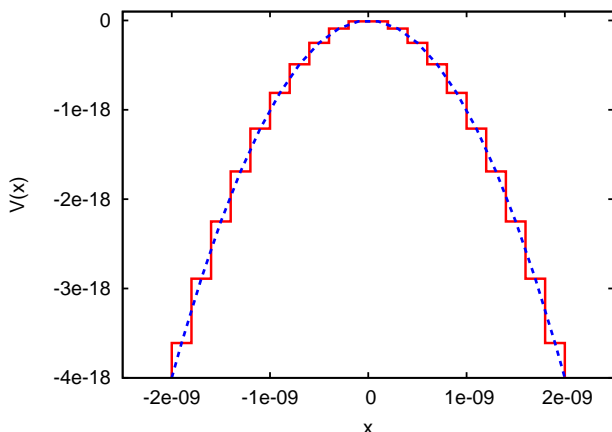


FIG. 1: The potential energy  $V(x) = -x^2$  (dashed line) approximated by steps.

Let us consider a potential  $V(x)$  which is divided into  $N$  segments as shown in Fig.(1) and let the computational domain be  $[x_0, x_N]$ . Thus, in Fig. 1,  $x_0 = -2nm$  and  $x_N = 2nm$ . The potential is approximated by a multistep function

$$V(x) = V_j = V[(x_{j-1} + x_j)/2] \quad (14)$$

for  $x_{j-1} < x < x_j$ ,  $j = 1, 2, \dots, N$ . The wave function  $\psi_j$  in the  $j$ th region for an electron with energy  $E$  is given by  $\psi_j(x) = A_j e^{ik_j x} + B_j e^{-ik_j x}$  where  $k_j = \sqrt{2m(E - V_j)} / \hbar$  for  $j = 1, \dots, N$  and  $\hbar = h/2\pi$ ,  $h$  being Planck's constant. Consider a first order WKB wavefunction to the left of the computational domain

$$\psi_0^{wkb}(x \leq x_0) = \frac{A_0}{\sqrt{\hbar k_0}} e^{i \int^x k(x') dx'} + \frac{B_0}{\sqrt{\hbar k_0}} e^{-i \int^x k(x') dx'} \quad (15)$$

with  $k_0 = \sqrt{2m(E - V(x_0))} / \hbar$  and a plane wave as the wavefunction for the first step of the potential

$$\psi_1(x) = A_1 e^{ik_1 x} + B_1 e^{-ik_1 x}. \quad (16)$$

Applying continuity of the wavefunction and its derivative at the boundary  $x = x_0$  we get,

$$\left( \frac{A_0}{\sqrt{\hbar k_0}} e^{i \int^x k(x') dx'} + \frac{B_0}{\sqrt{\hbar k_0}} e^{-i \int^x k(x') dx'} \right)_{x=x_0} = (A_1 e^{ik_1 x} + B_1 e^{-ik_1 x})_{x=x_0} \quad (17)$$

and

$$\begin{aligned} & \left[ \frac{A_0}{\sqrt{\hbar k_0}} \left( ik_0 - \frac{1}{2} \frac{k'_0}{k_0} \right) e^{i \int^x k(x') dx'} \right]_{x=x_0} + \\ & \left[ \frac{B_0}{\sqrt{\hbar k_0}} \left( -ik_0 - \frac{1}{2} \frac{k'_0}{k_0} \right) e^{-i \int^x k(x') dx'} \right]_{x=x_0} \\ & = ik_1 (A_1 e^{ik_1 x} - B_1 e^{-ik_1 x})_{x=x_0}. \end{aligned} \quad (18)$$

Choosing the reference point (lower limit) for the integration to be  $x_0$  itself,  $\int^{x_0} k(x') dx' = 0$ . Thus, from the above equations one can write the transfer matrix for the left boundary as

$$M_0 = \frac{1}{2\sqrt{\hbar k_0}} \begin{bmatrix} (1 + \gamma_0^+) e^{-ik_1 x_0} & (1 - \gamma_0^-) e^{-ik_1 x_0} \\ (1 - \gamma_0^+) e^{ik_1 x_0} & (1 + \gamma_0^-) e^{ik_1 x_0} \end{bmatrix} \quad (19)$$

where  $\gamma_0^- = \alpha_0 - \beta_0$ ,  $\gamma_0^+ = \alpha_0 + \beta_0$ ,  $\alpha_0 = k_0/k_1$  and  $\beta_0 = ik'_0/(k_0 k_1)$  with  $k'_0 = -mV'(x_0)/(k_0 \hbar^2)$ .

From the continuity equations at the boundaries of successive segments, the value of  $A_j$  and  $B_j$  can be reduced to a multiplication of the  $j$  ( $2 \times 2$ ) matrices

$$\begin{pmatrix} A_j \\ B_j \end{pmatrix} = \prod_{l=0}^{j-1} M_l \begin{pmatrix} A_0 \\ B_0 \end{pmatrix} \quad (20)$$

where

$$M_l = \frac{1}{2} \begin{bmatrix} (1 + \alpha_l)e^{-i(k_{l+1}-k_l)x_l} & (1 - \alpha_l)e^{-i(k_{l+1}+k_l)x_l} \\ (1 - \alpha_l)e^{i(k_{l+1}+k_l)x_l} & (1 + \alpha_l)e^{i(k_{l+1}-k_l)x_l} \end{bmatrix} \quad (21)$$

where  $\alpha_l = k_l/k_{l+1}$ ,  $l = 1, \dots, N-1$ . At the right end of the computational domain (i.e.  $x = x_N$ ), the WKB wavefunction takes the form

$$\begin{aligned} \psi_{N+1}(x = x_N) &= \frac{A_{N+1}}{\sqrt{\hbar k_{N+1}}} e^{i \int^x k(x') dx'} \\ &+ \frac{B_{N+1}}{\sqrt{\hbar k_{N+1}}} e^{-i \int^x k(x') dx'} \end{aligned} \quad (22)$$

with  $k_{N+1} = \sqrt{2m(E - V(x_N))} / \hbar$ . For  $x_{N-1} \leq x \leq x_N$ , the wavefunction is given by

$$\psi_N(x) = A_N e^{ik_N x} + B_N e^{-ik_N x}. \quad (23)$$

On applying continuity equations at the right boundary  $x = x_N$ , it follows that

$$\begin{aligned} (A_N e^{ik_N x} + B_N e^{-ik_N x})_{x=x_N} &= \\ \left( \frac{A_{N+1}}{\sqrt{\hbar k_{N+1}}} e^{i \int^x k(x') dx'} + \frac{B_{N+1}}{\sqrt{\hbar k_{N+1}}} e^{-i \int^x k(x') dx'} \right)_{x=x_N} \end{aligned} \quad (24)$$

and

$$\begin{aligned} ik_N (A_N e^{ik_N x} - B_N e^{-ik_N x})_{x=x_N} &= \\ \left[ \frac{A_{N+1}}{\sqrt{\hbar k_{N+1}}} e^{i \int^x k(x') dx'} \left( ik_{N+1} - \frac{1}{2} \frac{k'_{N+1}}{k_{N+1}} \right) \right]_{x=x_N} &+ \\ \left[ \frac{B_{N+1}}{\sqrt{\hbar k_{N+1}}} e^{-i \int^x k(x') dx'} \left( -ik_{N+1} - \frac{1}{2} \frac{k'_{N+1}}{k_{N+1}} \right) \right]_{x=x_N} &. \end{aligned} \quad (25)$$

The phase factors  $e^{\pm i \int^x k(x') dx'}$  can be absorbed in the coefficients  $A_{N+1}$  and  $B_{N+1}$  since their absolute value determines the transmission coefficient. Thus, from the above continuity equations, one can write the transfer matrix,  $M_N$ , for the right boundary as

$$\frac{\sqrt{\hbar}}{2i\sqrt{k_{N+1}}} \begin{bmatrix} (iS_N^+ + R_N)e^{ik_N x_N} & (iS_N^- + R_N)e^{-ik_N x_N} \\ (iS_N^- - R_N)e^{ik_N x_N} & (iS_N^+ - R_N)e^{-ik_N x_N} \end{bmatrix} \quad (26)$$

where  $S_N^+ = k_{N+1} + k_N$ ,  $S_N^- = k_{N+1} - k_N$ ,  $R_N = k'_{N+1}/2k_{N+1}$  and  $k'_{N+1} = -mV'(x_N)/(k_{N+1}\hbar^2)$ .

Let us consider the amplitude of the incident wave  $A_0 = 1$  and the final reflected wave  $B_{N+1} = 0$ . Therefore the transmission amplitude  $A_{N+1}$  is given as

$$A_{N+1} = \frac{\det(M_0) \det(M_1) \dots \det(M_N)}{M_{22}} \quad (27)$$

$$= \frac{k_1}{k_N} \frac{\det(M_0) \det(M_N)}{M_{22}} \quad (28)$$

where

$$M = \begin{pmatrix} M_{11} & M_{12} \\ M_{21} & M_{22} \end{pmatrix} = \prod_{k=0}^N M_k. \quad (29)$$

The transmission probability  $TC$  is thus

$$TC = |A_{N+1}|^2. \quad (30)$$

### C. Numerical Results

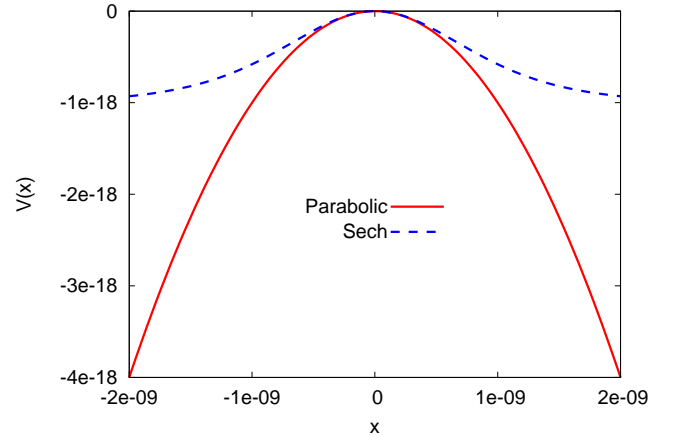


FIG. 2: The Parabolic potential,  $V(x) = -x^2$  (solid line) and the secant hyperbolic (Sech) potential  $V(x) = V_0(\text{sech}^2(x/x_0) - 1)$  (dashed line) within the computational domain  $[-2\text{nm}, 2\text{nm}]$ . Here  $V_0 = 1 \times 10^{-18}\text{J}$  and  $x_0 = 1 \times 10^{-9}\text{m}$ .

We present results for two potentials  $V(x) = -x^2$  and  $V(x) = V_0(\text{sech}^2(x/x_0) - 1)$ ,  $V_0 = 1 \times 10^{-18}\text{J}$ ,  $x_0 = 1 \times 10^{-9}\text{m}$  (see Fig. 2), for which the exact transmission coefficients are known [8] (see Fig. 3). The computational domain used is from  $[-2\text{nm}, 2\text{nm}]$  while the energy range over which the transmission coefficient varies from 0 to 1 is  $-2 \times 10^{-19}\text{J}$  to  $2 \times 10^{-19}\text{J}$ . The two potentials are shown in Fig. (2). While the parabolic potential rapidly decreases for  $|x| > 0$ , the slope of the secant hyperbolic potential decreases for increasing  $|x|$  with a saturation value  $V(\pm\infty) = -1 \times 10^{-18}$ . It can thus be expected

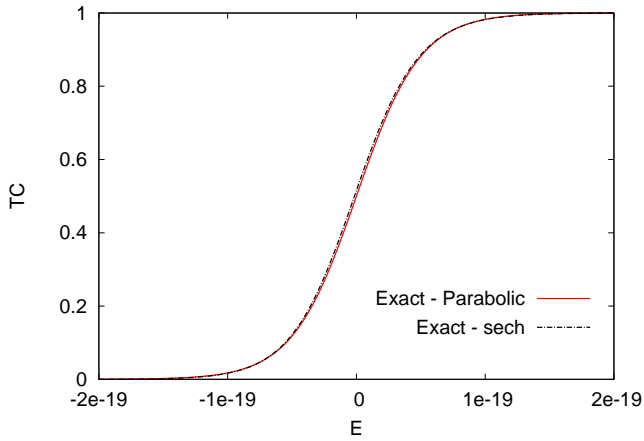


FIG. 3: Transmission coefficient (TC) for the parabolic (solid) and secant hyperbolic potentials (dashed). The energy range covers the variation of TC from 0 to 1.

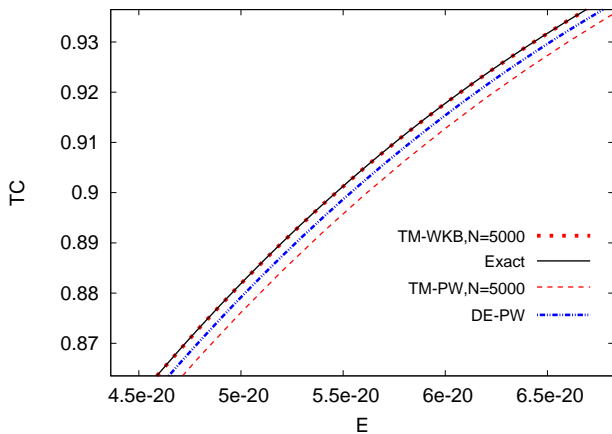


FIG. 4: A comparison of transmission coefficient obtained by four numerical methods along with the exact result for the parabolic potential  $V(x) = -x^2$ . The DE method using WKB boundary condition is hard to distinguish from the exact or TM-WKB results and is therefore not shown. The transfer matrix methods are labelled TM. The DE-PW (middle curve) fares better than TM-PW. The solid line is the exact result.

that with a computational domain  $|x| \leq 2 \times 10^{-9}$  m, the plane wave method for the secant hyperbolic potential should fare reasonably well alongside the WKB methods. Unless otherwise mentioned, all distances plotted are in metres and energy (including potential  $V(x)$ ) in joule.

In Fig. (4), we present a comparison of the numerical methods discussed along with the exact result. Two of these use the differential equation (DE) approach where the Schrödinger equation is solved but with plane and WKB waves respectively at the boundary of the computational domain. The other two are the transfer matrix methods (TM), again with plane and WKB waves at the boundary of the computational domain. The TM and DE methods with WKB boundary condition are clearly

the best (DE-WKB is not shown in the figure since it is indistinguishable from TM-WKB and the exact result). The Plane Wave (PW) methods have errors with DE-PW better than TM-PW method.

The improvement with WKB boundary conditions in both the DE and TM methods however depends on the energy under consideration. We have thus computed the relative error using the exact result for both potentials. These are plotted in Figs. (5) and (6) for the parabolic and secant hyperbolic potentials respectively.

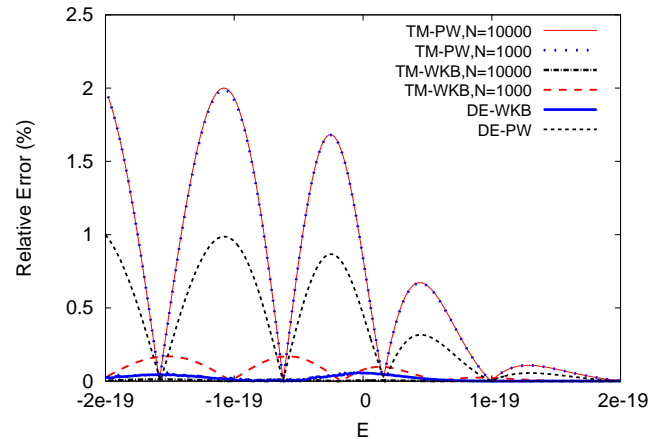


FIG. 5: Relative error in transmission coefficient for the parabolic potential for the four numerical methods discussed above. The largest errors are in the TM-PW method (top two) followed by the DE-PW method.

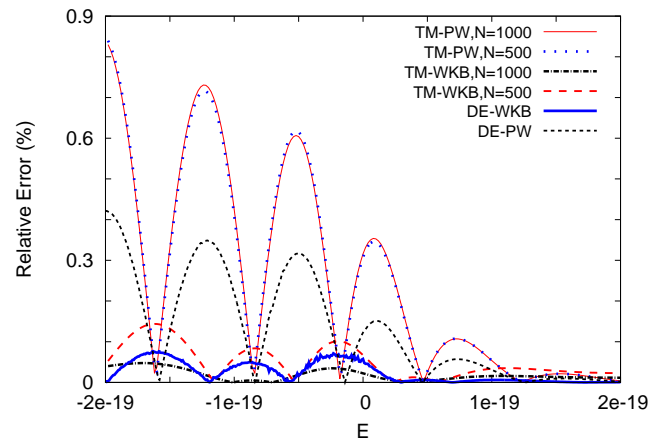


FIG. 6: Relative error in transmission coefficient for the secant hyperbolic potential as in Fig. 5.

Note that for the TM-PW method, the error saturates fast with  $N$  for both potentials whereas for the TM-WKB method, the error is seen to reduce with  $N$ . Also, both the TM-WKB and DE-WKB methods perform much better than the plane wave counterparts at all energies with the TM method outperforming the DE method for a few thousand steps ( $N$ ). Note that for the secant hyperbolic

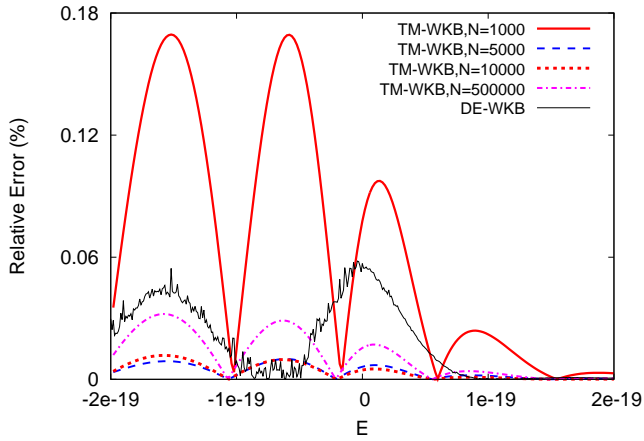


FIG. 7: Relative error in transmission coefficient for the parabolic potential for TM-WKB method with different values of  $N$ . Also shown is the DE-WKB result (irregular solid curve) for comparison.

potential, a reduced computational domain (for instance  $|x| \leq 1\text{nm}$ ), leads to a greater improvement for the WKB methods over the plane-wave methods as expected.

Finally, we compare the error in the TM-WKB method as the number of steps,  $N$ , is increased. This is shown in Fig. 7 for the parabolic potential. The error reduces initially as  $N$  is increased but beyond  $N = 5000$ , the error grows slightly before saturating at around  $N = 10^5$  to values that are still lower than the DE-WKB method. The energy-averaged error for the saturated TM-WKB method is about 65 times less than the saturated TM-PW method for  $N = 10^5$ .

### III. HIGHER ORDER WKB

In the previous section, a first order WKB wavefunction was used to determine non-reflecting boundary conditions at the edge of the computational domain resulting in considerable improvement of accuracy in the transmission coefficient.

The method can be easily generalized to achieve higher order WKB boundary conditions. We shall, however, restrict ourselves to third order WKB wavefunctions in much of what follows and show that the transfer matrix formalism can be modified further to achieve orders of magnitude improvement in accuracy over the first order TM results.

On using the usual WKB expansion for the wavefunction  $\psi(x) = e^{\frac{i}{\hbar}S(x)}$  with  $S(x) = \sum_{n=0}^{\infty} \hbar^n S_n$ , the Schrödinger equation yields the following equations for  $S'_n(x)$ :

$$S'_0 = \pm p(x) \quad (31)$$

$$S'_1 = \frac{i}{2} \frac{p'(x)}{p(x)} \quad (32)$$

$$S'_2 = \pm \left[ -\frac{p''(x)}{4p^2(x)} + \frac{3(p'(x))^2}{8p^3(x)} \right] \quad (33)$$

$$S'_3 = -\frac{ip'''(x)}{8p^3(x)} + \frac{i3p'(x)p''(x)}{4p^4(x)} - \frac{i3(p'(x))^3}{4p^5(x)} \quad (34)$$

where  $p(x) = \sqrt{2m(E - V(x))}$ . The first two terms  $S_0(x) = \pm \int^x p(x')dx'$  and  $S_1(x) = (i/2) \ln |p(x)|$  give rise to the first order WKB wavefunction used in the previous section.

Note the terms are alternately real and imaginary. Thus  $S_0$  and  $S_2$  give rise to a phase while  $S_1$  and  $S_3$  contribute to the amplitude. Further,  $S_0$  and  $S_2$  can assume positive or negative values depending on the sign of the momentum  $p(x)$ . A standard right moving can thus be expressed as  $\psi_+(x) = e^{\frac{i}{\hbar}S_i(x)}$  while a left moving wave can be expressed as  $\psi_-(x) = e^{\frac{i}{\hbar}S_r(x)}$  where

$$S_i(x) = +S_0(x) + \hbar S_1(x) + \hbar^2 S_2(x) + \hbar^3 S_3(x) \quad (35)$$

$$S_r(x) = -S_0(x) + \hbar S_1(x) - \hbar^2 S_2(x) + \hbar^3 S_3(x). \quad (36)$$

A general third order WKB wavefunction at the left end of the computational domain is thus

$$\psi_0(x) = A_0 e^{iS_i(x)/\hbar} + B_0 e^{iS_r(x)/\hbar}. \quad (37)$$

In the transfer matrix formalism, the matrix  $M_0$  is thus

$$M_0 = \begin{bmatrix} \left(1 + \frac{S'_i}{\hbar k_1}\right) e^{i(\frac{S_i}{\hbar} - k_1 x_0)} & \left(1 + \frac{S'_r}{\hbar k_1}\right) e^{i(\frac{S_r}{\hbar} - k_1 x_0)} \\ \left(1 - \frac{S'_i}{\hbar k_1}\right) e^{i(\frac{S_i}{\hbar} + k_1 x_0)} & \left(1 - \frac{S'_r}{\hbar k_1}\right) e^{i(\frac{S_r}{\hbar} + k_1 x_0)} \end{bmatrix} \quad (38)$$

where  $S_i$ ,  $S_r$ ,  $S'_i$  and  $S'_r$  are evaluated at  $x_0$ . Similarly, the wavefunction at the right end is

$$\psi_{N+1}(x) = A_{N+1} e^{iS_i(x)/\hbar} + B_{N+1} e^{iS_r(x)/\hbar} \quad (39)$$

so that the transfer matrix  $M_N$  is

$$M_N = \frac{1}{S'_i - S'_r} \begin{bmatrix} (\hbar k_N - S'_r) e^{i\alpha_i^+} & -(\hbar k_N + S'_r) e^{i\alpha_i^-} \\ -(\hbar k_N - S'_i) e^{i\alpha_r^+} & (\hbar k_N + S'_i) e^{i\alpha_r^-} \end{bmatrix} \quad (40)$$

where  $\alpha_i^+ = +k_N x - S_i/\hbar$ ,  $\alpha_i^- = -k_N x - S_i/\hbar$ ,  $\alpha_r^+ = +k_N x - S_r/\hbar$  and  $\alpha_r^- = -k_N x - S_r/\hbar$ . Here  $S_i, S_r, S'_i$  and  $S'_r$  are evaluated at  $x_N$ .

As before, with  $A_0 = 1$  and  $B_{N+1} = 0$ , the amplitude

$$A_{N+1} = \frac{k_1}{k_N} \frac{\det(M_0) \det(M_N)}{M_{22}} \quad (41)$$

with  $M = \prod_{l=0}^N M_l$ , where  $M_0$  and  $M_N$  are given by Eqns. (38) and (40) respectively while for other values of  $l$ ,  $M_l$  is given by Eq. (21).

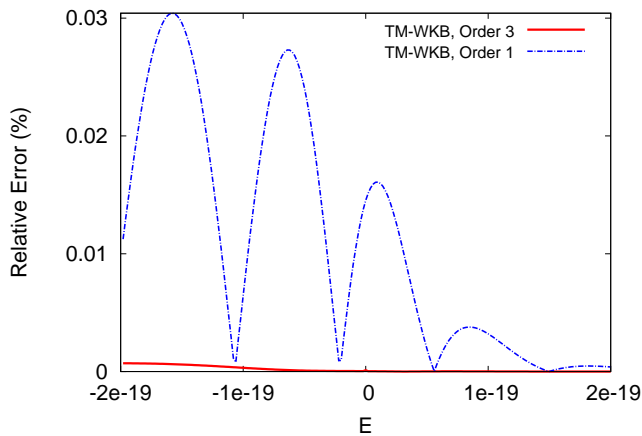


FIG. 8: Relative error in transmission coefficient for the parabolic potential using the transfer matrix method with 1<sup>st</sup> (dashed) and 3<sup>rd</sup> (continuous) order WKB boundaries.

The incident and transmitted currents can be expressed respectively as

$$J_{IN} = \frac{|A_0|^2}{2m} 2\Re(S'_i(x_0)) e^{-\frac{2}{\hbar}\Im(S_i(x_0))} \quad (42)$$

$$J_{TR} = \frac{|A_{N+1}|^2}{2m} 2\Re(S'_i(x_N)) e^{-\frac{2}{\hbar}\Im(S_i(x_N))} \quad (43)$$

where  $\Re$  and  $\Im$  denote the real and imaginary part respectively. The transmission coefficient  $TC = J_{IN}/J_{TR}$  is thus

$$TC = |A_{N+1}|^2 \frac{\Re(S'_i(x_N))}{\Re(S'_i(x_0))} e^{\frac{2}{\hbar}(\Im(S_i(x_0)) - \Im(S_i(x_N)))} \quad (44)$$

since  $A_0 = 1$ .

In order to check whether higher order terms improve the accuracy of the transmission coefficient, we consider

the parabolic potential  $V(x) = -x^2$ . For convenience, we consider the reference point for integrating Eqns. (34) as the left boundary ( $x = x_0$ ) of the computational domain so that  $S_n(x_0) = 0$  for  $n = 0, 1, 2, 3$ . Using  $p(x) = \sqrt{2m(E + x^2)}$ , Eqns. (34) can be integrated to obtain  $S_n(x_N)$ .

In Fig. 8, the transmission coefficient obtained using first and third order WKB boundary conditions are compared for  $N = 10^5$  at which both results converge [16]. Our results are shown in Fig. 8. The energy averaged improvement in relative error over the first order WKB result is 63 times while the average improvement over the plane wave method is about 4100 times.

#### IV. SUMMARY AND CONCLUSIONS

We have demonstrated that the use of WKB wavefunctions at the boundary of the computational domain improves the evaluation of the transmission coefficient enormously. For the parabolic potential, the error reduces by a factor of 4100 using third order transfer matrix method over the usual plane wave TM method.

It is important to note that the errors are largest at lower energies. This has significance in field emission calculations where the supply function may have large contributions below the Fermi level. The transfer matrix method with WKB boundary condition (TM-WKB) may thus be adopted due to the ease of implementation and the improvement in accuracy. Finally, the method can be directly generalized to multi-dimensional systems when the potential is separable.

#### V. ACKNOWLEDGEMENTS

The authors acknowledge stimulating discussions with Dr. Raghendra Kumar.

---

[1] R. H. Fowler and L. Nordheim, Proc. R. Soc. A **119**, 173 (1928).  
 [2] D. Biswas and R. Kumar, J. App. Phys. **115**, 114302 (2014).  
 [3] C. Jirauschek and T. Kubis, Appl. Phys. Rev. **1**, 011307 (2014).  
 [4] D. Vasileska and S. M. Goodnick (Eds.) *Nano-Electronic Devices: Semiclassical and quantum transport modeling*, Springer (2011).  
 [5] A. M. Ionescu and H. Riel, Nature **479**, 329 (2011).  
 [6] E. Cassan, J. App. Phys. **87**, 7931 (2000).  
 [7] L. Mao, C. Tan and M. Xu, Microelectronics Reliability **41**, 927 (2001).  
 [8] L. D. Landau and E. M. Lifshitz, *Quantum Mechanics*,

Pergamon Press, 3rd Ed. (1991).  
 [9] R. L. Jaffe, Am. J. Phys **78**, 620 (2010).  
 [10] Y. Ando and T. Itoh, J. App. Phys. **61**, 1497 (1987).  
 [11] C. Jirauschek, IEEE J. Quant. Elec., **45**, 1059 (2009).  
 [12] The approximation is also used in the continued fraction method [13] for determining the transmission coefficient.  
 [13] J. P. Vigneron and Ph Lambin, J. Phys. **A13**, 1135 (1980).  
 [14] D. Biswas and R. Kumar, Eur. Phys. J. B **85** 189 (2012).  
 [15] D. Biswas and R. Kumar, Europhys. Lett. **102**, 58002 (2013).  
 [16] The third order WKB transfer matrix method converges faster than the first order method.